Infectious Agents and Cancer

BRIEF REPORT Open Access

Microbiota and metabolite profiles of saliva, oral swab and cancer tissue from patients with oral squamous cell carcinoma (OSCC)

Kailiu Wu[1,2†], Beihui Xu[1†], Xinyu Zhou[1,2], Haiyan Guo[1], Guanhuan Du[3], Chenping Zhang[2*], Fuxiang Chen[1,4*] and Xu Chen[1*]

Abstract

Oral squamous cell carcinoma (OSCC) was the most common malignant type of head and neck squamous cell carcinoma (HNSCC) with a low survival rate. The microbiota in oral cavity or tumor tissues may play a critical role in the OSCC. In this study, we characterized the microbiota from oral cancer tissues, oral swabs and saliva of patients with OSCC using 16S rRNA sequencing. We found differential profiles and amounts of microbiota in oral cancer tissues compared with adjacent tissues, as well as in oral swabs and saliva from OSCC patients compared with healthy individuals. *Fusobacterium nucleatum* and *Porphyromonas endodontalis* were found increased in cancer tissues and saliva from OSCC patients. *Prevotella melaninogenica* was found increased in the saliva and oral swabs from OSCC patients. These data suggested that microbiota varied according to different samples. Kyoto Encyclopedia of Genes and Genomes (KEGG) analysis indicated an important role of metabolic pathways in the interaction between microbiota and cancers. Then we analyzed the metabolites from cancer tissues and saliva of OSCC patients by liquid chromatograph-mass spectrometry/mass spectrometry (LC-MS/MS) and gas chromatograph-mass spectrometry (GC-MS). Differential profiles of metabolites were also observed in the cancer tissues compared with adjacent tissues and in the saliva from OSCC patients compared with healthy individuals. It showed that denticulaflavonol was significantly increased while D-mannose was significantly decreased in both cancer tissues and saliva of OSCC patients. Taken together, these results suggested an association between microbiota/metabolites (such as *Fusobacterium* and mannose) and OSCC, in which the molecular mechanism need further investigated.

Keywords Microbiota, Metabolite, OSCC, Saliva, Oral swab, Oral cancer

†Kailiu Wu and Beihui Xu contributed equally to this work.

*Correspondence:
Chenping Zhang
zhang.chenping@hotmail.com
Fuxiang Chen
chenfx@sjtu.edu.cn
Xu Chen
chenxu917@shsmu.edu.cn

[1]Department of Laboratory Medicine, Shanghai Ninth People's Hospital, Shanghai Jiao Tong University School of Medicine, Shanghai, China
[2]Department of Oral and Maxillofacial-Head and Neck Oncology, Shanghai Ninth People's Hospital, Shanghai Jiao Tong University School of Medicine, Shanghai, China
[3]Department of Oral Mucosal Diseases, Shanghai Ninth People's Hospital, Shanghai Jiao Tong University School of Medicine, Shanghai, China
[4]Faculty of Medical Laboratory Science, College of Health Science and Technology, Shanghai Jiao Tong University School of Medicine, Shanghai, China

Introduction

Head and neck squamous cell carcinoma (HNSCC) was one of the main cancer types worldwide, and oral squamous cell carcinoma (OSCC) was the most common malignant cancer of HNSCC [1]. In spite of multiple therapeutic approaches, the five-year survival rate of OSCC was still low [2]. There were environmental, genetic and epigenetic factors influencing the progression and prognosis of OSCC, including the microbiota in the oral cavity and tumor tissues [2–4]. It has been reported that some specific bacteria were associated with OSCC such as *Fusobacterium nucleatum* (Fnu), *Porphyromonas gingivalis* (Pgi) and *Prevotella melaninogenica* (Pme) [4–7]. A critical role of Fnu in the progression and chemoresistance of colorectal cancer (CRC) has been elucidated [8–11], while the role of Fnu in oral cancer, especially OSCC, was relatively less understood. Fnu could enhance the proliferation of OSCC via E-cadherin/β-catenin pathway and Ku70/p53 pathway [12, 13], and Fnu infection could promote the invasion of oral cancer cells by partial-epithelial mesenchymal transition (p-EMT) [14]. Recently, it was found that Fnu outer membrane vesicles (OMVs) contribute to the metastasis of oral cancer through activating autophagy [15]. The interaction between microorganisms and other cells within the tumor microenvironment would also affect the OSCC development [16–21]. For example, Pgi promoted the immune evasion of OSCC by affecting macrophage [21]. Therefore, having a knowledge of microbiota and metabolites within and surrounding oral cancers would contribute to understanding the pathogenesis of OSCC.

Materials and methods

Study design

The oral cancer tissues and adjacent normal tissues from patients with oral squamous cell carcinoma (OSCC) were collected to explore the tissue microbiota by 16S rRNA sequencing. The saliva and oral swabs from OSCC patients and healthy individuals were also collected to detect the oral microbiota. The participants had no antibiotic use in the past one month before sampling. Moreover, analysis of metabolites from cancer tissues compared with adjacent normal tissues and saliva from OSCC patients compared with healthy individuals was performed by liquid chromatograph-mass spectrometry (LC-MS/MS) and gas chromatograph-mass spectrometry (GC-MS). This study was approved by Shanghai Ninth People's Hospital Ethics Committee.

Sample collection

The oral cancer tissues and adjacent tissues were collected by sterile surgical instruments and frozen in sterile tubes at -80℃. These cancer tissues were collected from two different batches including 7 paired tissues in first batch and 9 paired ones in second batch. These 16 paired tissues from two batches were subjected to 16S rRNA sequencing, and the 9 paired tissues in second batch were also performed metabolite analysis by LC-MS/MS and GC-MS.

The saliva from patients with OSCC and healthy individuals were collected in sterile cup with cover and transferred into sterile tubes frozen at -80℃. A total of 13 saliva from patients and 13 saliva from healthy individuals were subjected to detect microbiota by 16S rRNA sequencing. Additionally, a total of 9 saliva from patients and 7 saliva from healthy individuals were subjected to metabolite analysis by LC-MS/MS and GC-MS.

The oral swabs from patients with OSCC and healthy individuals were collected and stored at -80℃. A total of 9 oral swabs from patients and 9 oral swabs from healthy individuals were subjected to detect microbiota by 16S rRNA sequencing.

16S rRNA sequencing

Total genomic DNA from tissues/saliva/oral swabs was extracted using DNA Extraction Kit following the manufacturer's instructions. Concentration of DNA was verified with NanoDrop and agarose gel. The genome DNA was used as template for PCR amplification with the barcoded primers and Tks Gflex DNA Polymerase (Takara). V3-V4 variable regions of 16S rRNA genes was amplified with universal primers 343F (5'-TACGGRAGGCAGCAG-3') and 798R (5'-AGGGTATCTAATCCT-3'). Amplicon quality was visualized using gel electrophoresis, purified with AMPure XP beads (Agencourt), and amplified for another round of PCR. After purified with the AMPure XP beads again, the final amplicon was quantified using Qubit dsDNA assay kit. Equal amounts of purified amplicon were pooled for subsequent sequencing. Raw sequencing data were in FASTQ format. Paired-end reads were then preprocessed using cutadapt software to detect and cut off the adapter. After trimming, paired-end reads were filtering low quality sequences, denoised, merged and detect and cut off the chimera reads using DADA2 with the default parameters of QIIME2 (2020.11). At last, the software output the representative reads and the amplicon sequence variant (ASV) abundance table. The representative read of each ASV was selected using QIIME2 package. All representative reads were annotated and blasted against Silva database Version 138 or Unite using q2-feature-classifier with the default parameters. The amplicon sequencing and analysis were conducted by OE biotech Co., Ltd. (Shanghai, China).

LC-MS/MS

Tissues or saliva stored at -80℃ were thawed at room temperature. 30 mg tissues or 100 μL saliva was added to

a 1.5 mL Eppendorf tube with L-2-chlorophenylalanine (0.06 mg/mL) dissolved in methanol as internal standard, and the tube was vortexed. Subsequently, ice-cold mixture of methanol and acetonitrile was added, and the mixtures were vortexed for 1 min, and the whole samples were extracted by ultrasonic for 10 min in ice-water bath, stored at -20 ℃ for 30 min. The extract was centrifuged at 4 °C (13000 rpm) for 10 min. 120 μL of supernatant in a glass vial was dried in a freeze concentration centrifugal dryer. Also, the mixture of methanol and water (1/4, vol/vol) were added to each sample, samples vortexed for 30 s, extracted by ultrasonic for 3 min in ice-water bat, then placed at -20 °C for 2 h. Samples were centrifuged at 4 °C (13000 rpm) for 10 min. The supernatants (150 μL) from each tube were collected using crystal syringes, filtered through 0.22 μm microfilters and transferred to LC vials. The vials were stored at -80 °C until LC-MS analysis. QC samples were prepared by mixing aliquot of the all samples to be a pooled sample.

An ACQUITY UPLC I-Class plus (Waters Corporation, Milford, USA) fitted with Q-Exactive mass spectrometer equipped with heated electrospray ionization (ESI) source (Thermo Fisher Scientific, Waltham, MA, USA) was used to analyze the metabolic profiling in both ESI positive and ESI negative ion modes. An ACQUITY UPLC HSS T3 column (1.8 μm, 2.1 × 100 mm) were employed in both positive and negative modes. The binary gradient elution system consisted of (A) water (containing 0.1% formic acid, v/v) and (B) acetonitrile (containing 0.1% formic acid, v/v) and separation was achieved using the following gradient: 0.01 min, 5% B; 2 min, 5% B; 4 min, 30% B; 8 min, 50% B; 10 min, 80% B; 14 min, 100% B; 15 min, 100% B; 15.1 min, 5% and 16 min, 5%B. The flow rate was 0.35 mL/min and column temperature was 45℃. All the samples were kept at 10℃ during the analysis.

The original LC-MS data were processed by software Progenesis QI V3.0 (Nonlinear, Dynamics, Newcastle, UK) for baseline filtering, peak identification, integral, retention time correction, peak alignment, and normalization. Main parameters of 5 ppm precursor tolerance, 10 ppm product tolerance, and 5% product ion threshold were applied. Compound identification were based on precise mass-to-charge ratio (M/z), secondary fragments, and isotopic distribution using The Human Metabolome Database (HMDB), Lipidmaps (V2.3), Metlin, and self-built databases. The extracted data were then further processed by removing any peaks with a missing value (ion intensity = 0) in more than 50% in groups, by replacing zero value by half of the minimum value, and by screening according to the qualitative results of the compound. Compounds with resulting scores below 36 (out of 60) points were also deemed to be inaccurate and removed. A data matrix was combined from the positive and negative ion data. The metabolomic data analysis was performed by Shanghai Luming biological technology Co., Ltd (Shanghai, China).

GC-MS

Tissues or saliva stored at -80℃ were thawed at room temperature. 30 mg tissues or 100 μL saliva was added to a 1.5 mL Eppendorf tube with L-2-chlorophenylalanine (0.06 mg/mL) dissolved in methanol as internal standard, and the tube was vortexed for 10 s. Subsequently, ice-cold mixture of methanol and acetonitrile (2/1, vol/vol) was added, and the mixtures were vortexed for 30 s, and the whole samples were extracted by ultrasonic for 10 min in ice-water bath, stored at -20℃ for 30 min. The extract was centrifuged at 4 °C (13000 rpm) for 10 min. The supernatant in a glass vial was dried in a freeze concentration centrifugal dryer. An aliquot of the 120 μL supernatant was transferred to a glass sampling vial for vacuum-dry at room temperature. And 80 μL of 15 mg/mL methoxylamine hydrochloride in pyridine was subsequently added. The resultant mixture was vortexed vigorously for 2 min and incubated at 37 °C for 90 min. 50 μL of BSTFA and 20 μL n-hexane were added into the mixture, which was vortexed vigorously for 2 min and then derivatized at 70 °C for 60 min. The samples were placed at ambient temperature for 30 min before GC-MS analysis. QC samples were prepared by mixing aliquot of the all samples to be a pooled sample.

The derivatived samples were analyzed on an Agilent 7890B gas chromatography system coupled to an Agilent 5977 A MSD system (Agilent Technologies Inc., CA, USA). A DB-5MS fused-silica Capillary Column (30 m × 0.25 mm × 0.25 μm, Agilent J & W Scientific, Folsom, CA, USA) was utilized to separate the derivatives. Helium (> 99.999%) was used as the carrier gas at a constant flow rate of 1 mL/min through the column. The injector temperature was maintained at 260℃. The initial oven temperature was 60℃ held at 60 °C for 0.5 min, ramped to 125℃ at a rate of 8℃/min, to 210℃ at a rate of 5℃/min, to 270℃ at a rate of 10℃/min, to 305℃ at a rate of 20℃/min, and finally held at 305℃ for 5 min. The temperature of MS quadrupole and ion source (electron impact) was set to 150 and 230℃, respectively. The collision energy was 70 eV. Mass spectrometric data was acquired in a full-scan mode (m/z 50–500).

The obtained GC/MS raw data in.D format were transferred to.abf format via software Analysis Base File Converter for quick retrieval of data. Then, data were imported into software MS-DIAL, which performs peak detection, peak identification, MS2Dec deconvolution, characterization, peak alignment, wave filtering, and missing value interpolation. Metabolite characterization was based on LUG database. A data matrix was derived. The three-dimensional matrix includes: sample

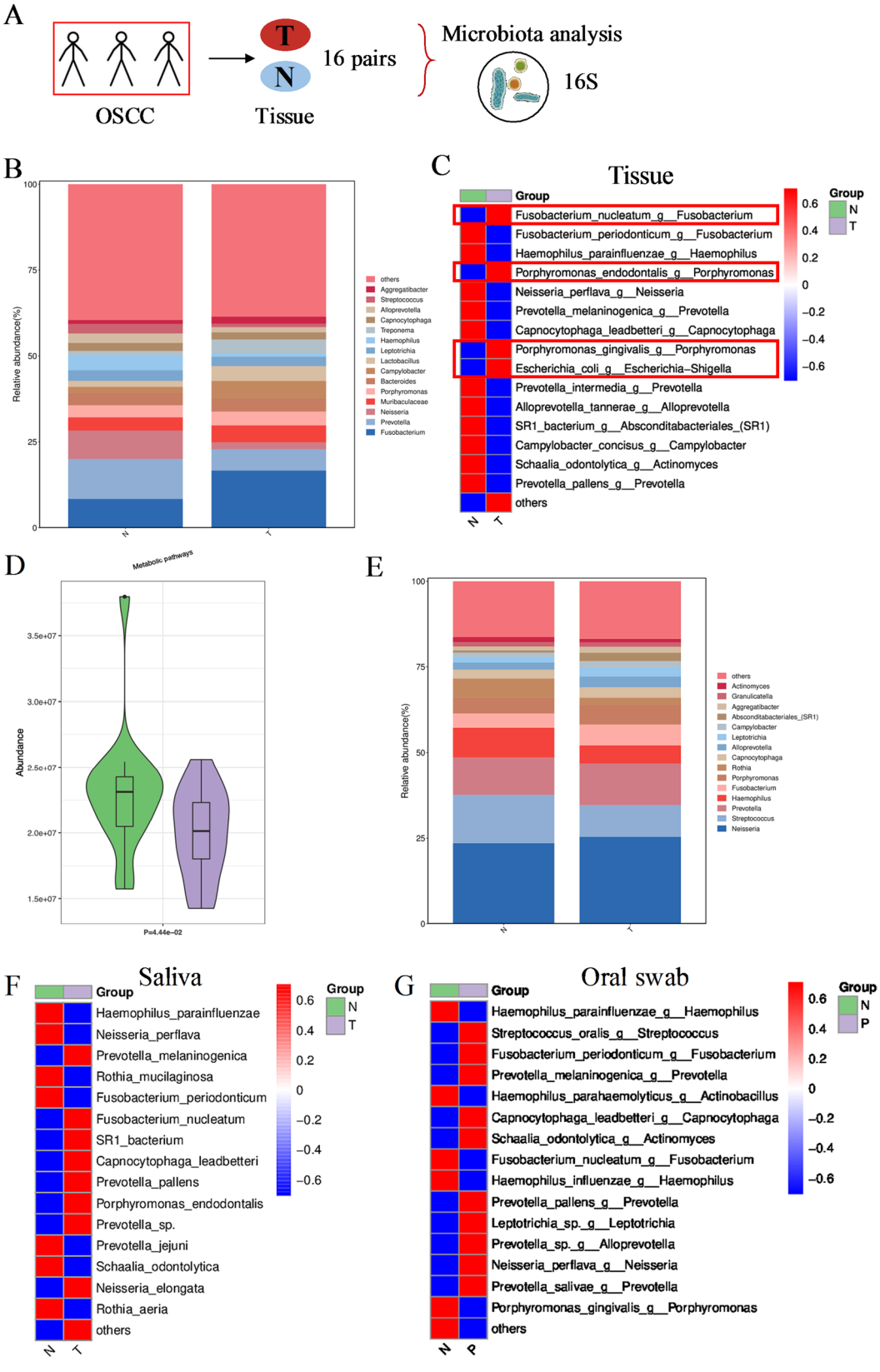

Fig. 1 (See legend on next page.)

(See figure on previous page.)

Fig. 1 Microbiota in cancer tissues, saliva and oral swabs from OSCC patients. **(A)** Scheme diagram of microbiota analysis in cancer tissues and adjacent tissues from OSCC patients. **(B)** Relative abundance of bacteria in cancer tissues and adjacent tissues at the genus level ($n = 16$); N, adjacent tissues, T, cancer tissues. **(C)** Heatmap of bacteria in cancer tissues and adjacent tissues at the species level ($n = 16$); N, adjacent tissues, T, cancer tissues. **(D)** KEGG analysis based on the data of 16S rRNA from cancer tissues and adjacent tissues from OSCC patients. **(E)** Relative abundance of bacteria in saliva at the genus level ($n = 13$); N, healthy individuals, T, OSCC patients. **(F)** Heatmap of bacteria in saliva at the species level ($n = 13$); N, healthy individuals, T, OSCC patients. **(G)** Heatmap of bacteria from oral swabs at the species level ($n = 9$); N, healthy individuals, P, OSCC patients

information, the name of the peak of each substance, retention time, retention index, mass-to-charge ratio, and signal intensity. In each sample, all peak signal intensities were segmented and normalized according to the internal standards with RSD < 0.1 after screening. After the data was normalized, redundancy removal and peak merging were conducted to obtain the data matrix. The metabolomic data analysis was performed by Shanghai Luming biological technology Co., Ltd (Shanghai, China).

Statistical analysis

For 16S rRNA sequencing, the quality control of raw reads was performed to gain clean tags. And the clean tags were filtered, denoised and cleaned off the chimera reads to get the valid tags. The valid tags were normalized and shown in ASV abundance tables. The community structure of bacteria was shown by barplot at top 15 genus levels and shown by heatmap at top 15 species levels. The barplot at top 15 genus levels and the heatmap at top 15 species levels between the oral cancer tissues and adjacent tissues were compared using t-test or Wlicoxon test. The heatmaps at top 15 species levels of saliva and oral swabs between OSCC patients and healthy individuals were also compared using t-test or Wlicoxon test. Kyoto Encyclopedia of Genes and Genomes (KEGG) analysis based on 16S rRNA data between the oral cancer tissues and adjacent tissues was conducted and compared using t-test, and top fifteen KEGG pathways were displayed.

For analysis of metabolites, internal quality control samples were included for LC-MS/MS and GC-MS quality control. Principle component analysis (PCA) was used to evaluated and assessed for the quality. A two-tailed Student's t-test was further used to verify whether the metabolites of difference between two groups were significant. Differential metabolites were selected with VIP values greater than 1.0 and p-values less than 0.05. Differential metabolites were further used to for KEGG pathway (http://www.genome.jp/kegg/) enrichment analysis.

Results and discussion

In this study, we firstly characterized the microbiota from oral cancer tissues vs. adjacent tissues, oral swabs and saliva from patients with OSCC. The raw reads of 16S rRNA data were subjected to quality control and the valid tags for ASV were shown in Table S1. We observed differential microbiota profiles between oral cancer tissues and adjacent normal tissues. A total of 16 paired tissues including oral cancer tissues and adjacent tissues were collected to detect the tissue microbiota by 16S rRNA sequencing. These tissues were subjected to detect in two different batches (7 paired tissues in first batch and 9 paired ones in second batch), and the data were combined for analysis as shown in Fig. 1A. The data demonstrated the presence of diverse bacteria such as *Neisseria*, *Prevotella* and *Fusobacterium* within the tissues from patients with OSCC (Fig. 1B). Interestingly, *Fusobacterium nucleatum*, which played a pro-tumor role in CRC, was more enriched in the cancer tissues compared with the adjacent tissues (Fig. 1C). Moreover, other bacteria including *Porphyromonas gingivalis* and *Porphyromonas endodontalis* were also more enriched in the cancer tissues. However, *Fusobacterium periodonticum* and *Prevotella melaninogenica* were more abundant in adjacent normal tissues (Fig. 1C). These results suggested that differential microbiota was enriched in the oral cancer tissues and adjacent normal tissues, pointing out an association between some bacteria and OSCC. By Kyoto Encyclopedia of Genes and Genomes (KEGG) analysis based on the data of 16S rRNA between the oral cancer tissues and adjacent normal tissues, metabolic pathways were among the top fifteen differential pathways (Fig. 1D and Figure S1A), indicating an important role of metabolic pathways in the interaction between microbiota and cancers. Recently, it has been reported that *Fnu*-derived OMVs could promote immunotherapy resistance in HNSCC via changes in tryptophan metabolism in tumor-associated macrophages [22], which further confirmed our findings.

Next, we explored the microbiota in the surrounding environment of oral cancer from saliva. Saliva from 13 OSCC patients and 13 healthy individuals were collected and analyzed, and raw reads and ASV were shown in Table S1. As shown in Fig. 1E, the oral indigenous flora such as *Neisseria* and *Streptococcus* were present in the saliva from both patients and healthy individuals. In addition, *Fusobacterium*, *Prevotella* and *Porphyromonas* were found in the saliva. Precisely, *Fusobacterium nucleatum*, *Prevotella melaninogenica* and *Porphyromonas endodontalis* were increased in the saliva from OSCC patients compared with those from healthy individuals (Fig. 1F). Similar bacteria including *Fusobacterium nucleatum* and *Porphyromonas endodontalis* were found increased in both cancer tissues and saliva from OSCC patients,

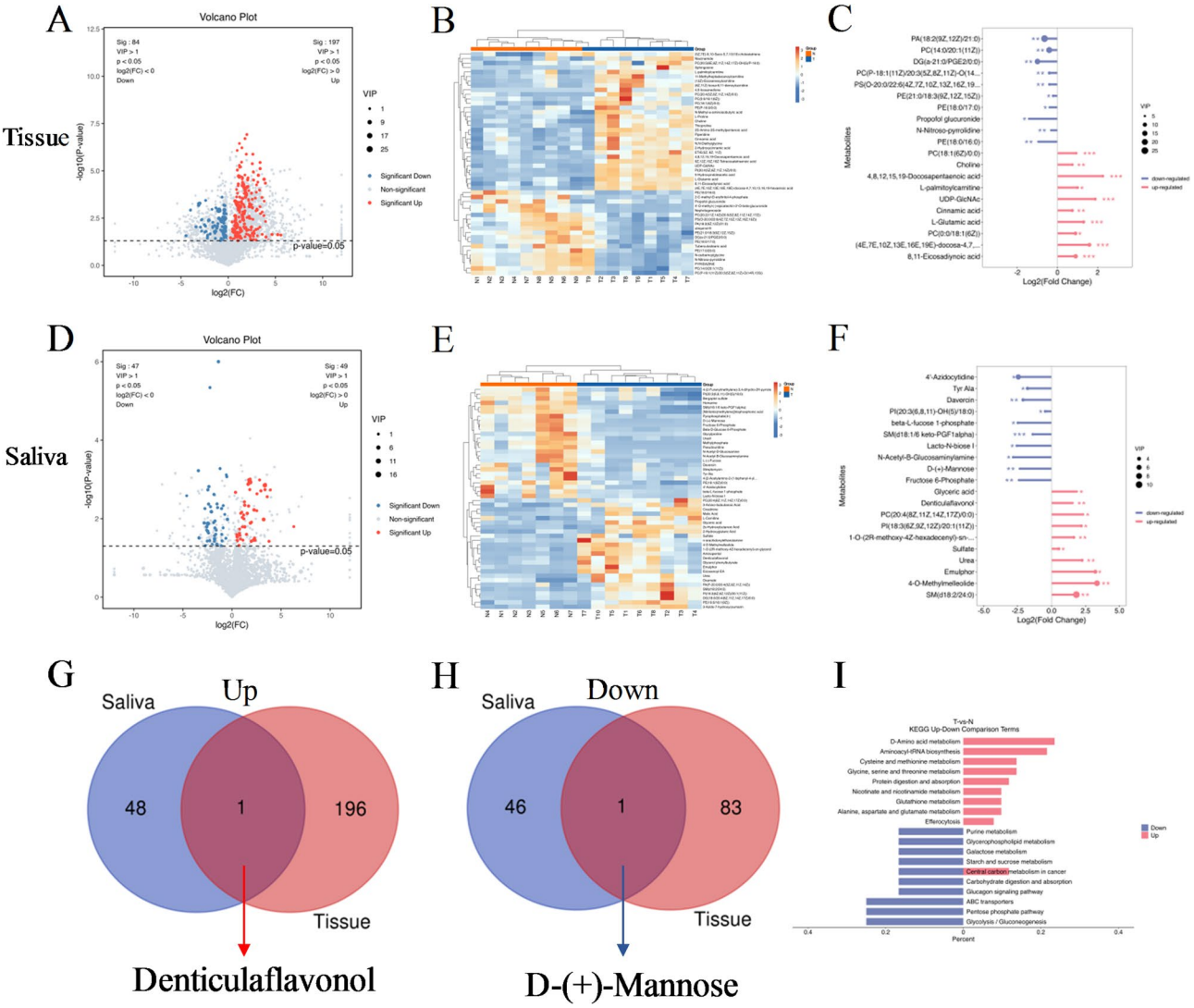

Fig. 2 Metabolites in cancer tissues and saliva from OSCC patients. **(A)** Volcano plot of metabolites from cancer tissues from OSCC patients by LC-MS/MS and GC-MS. **(B)** Heatmap of differential metabolites from cancer tissues from OSCC patients. **(C)** Top ten down-regulated and top ten up-regulated metabolites from cancer tissues compared with adjacent tissues. (A-C) $n = 9$; N, adjacent tissues, T, cancer tissues. **(D)** Volcano plot of metabolites from saliva by LC-MS/MS and GC-MS. **(E)** Heatmap of differential metabolites from saliva. **(F)** Top ten down-regulated and top ten up-regulated metabolites in saliva from OSCC patients compared with healthy individuals. **(D-F)** N, healthy individuals ($n = 7$), T, OSCC patients ($n = 9$). **(G)** Venn diagram of up-regulated metabolites in saliva and cancer tissues. **(H)** Venn diagram of down-regulated metabolites in saliva and cancer tissues. **(I)** KEGG analysis based on the differential metabolites in the cancer tissue (T) vs. adjacent tissues (N)

implying an association of these bacteria with OSCC. Then we also explored the microbiota in the surrounding environment of oral cancer using oral swab. Oral swabs from 9 OSCC patients and 9 healthy individuals were collected, and raw reads and ASV from oral swabs were also shown in Table S1. As shown in Fig. 1G, the differential microbiota profiles were found in oral swabs from OSCC patients and healthy individuals. *Fusobacterium nucleatum*, which was increased in cancer tissues and saliva from OSCC patients, was decreased in the oral swabs from OSCC patients (Fig. 1G). These data suggested that the relative amount of bacteria varied in different samples. A systematic study was needed to elucidate the difference of microbiota from different samples. All the data implied an association between microbiota such as *Fusobacterium nucleatum* and OSCC. However, there were some limitations of this study; The small sample size should be considered. Only 16 pairs of tissues,13 pairs of saliva and 9 pairs of oral swabs were collected and analyzed. A larger number of samples from participants need to be collected to confirm the findings of this preliminary study. And the association between microbiota and the progression, clinical stage and therapy outcome of OSCC need to be further investigated. Moreover, the causality between microbiota and OSCC need to be further explored by in-vitro experiments and animal models.

As shown in Fig. 1D and Figure S1A, the metabolic pathways may play a central role in the interaction between microbiota and OSCC. We finally performed the metabolomics analysis from cancer tissues and saliva by liquid chromatograph-mass spectrometry (LC-MS/MS) and gas chromatograph-mass spectrometry (GC-MS) as displayed in Fig. 2. The PCA of quality control (QC) and samples were displayed in Figure S1B and Figure S1C. The near clustering of quality controls demonstrated the good stability and repeatability of the experiments (Figure S1B-S1C). As shown in Fig. 2A and B, a total of 197 metabolites were significantly increased, while 84 metabolites were significantly decreased in the cancer tissues compared with the adjacent tissues. The top ten increased metabolites such as choline, and the top ten decreased metabolites were listed in Fig. 2C. Similarly, 49 metabolites were significantly increased, while 47 metabolites were significantly decreased in the saliva from OSCC patients compared with those from healthy individuals (Fig. 2D and F). Analysis of combined data from cancer tissues and saliva indicated that denticulaflavonol was significantly increased whereas D-(+)-mannose was significantly decreased in both cancer tissues and saliva (Fig. 2G and H). Moreover, KEGG analysis based on the differential metabolites in the cancer tissue compared with adjacent tissues suggested distinct metabolic pathways in the oral cancer tissues, including up-regulated D-amino acid metabolism and glycine/serine/threonine metabolism pathways and down-regulated purine metabolism and glycolysis pathways (Fig. 2I).

It has been reported that microbial metabolites play a critical role in human health and disease, including cancers [23–25]. There were many researches focusing on the gut microbial metabolites and cancers. In the gut, there were three main types of microbiota-derived metabolites, including metabolites produced by gut microbiota and those modified by gut microbiota from diet and host [23]. However, oral microbiota and their derived metabolites in oral cancer such as OSCC need to be explored. Similar to the metabolites in the gut, the oral microbiota-derived metabolites may contain the metabolites produced by oral microbiota and modified by oral microbiota from diet and host. For example, *Fusobacterium nucleatum* was found in the gut and oral cancer tissues. *Fusobacterium nucleatum*-derived succinic acid could induce resistance to immunotherapy in CRC [10]. We also detected enriched adenylsuccinic acid in the oral cancer tissues. However, its role in OSCC remain to be investigated. In the present study, we observed increased choline, docosapentaenoic acid, cinnamic acid and eicosadiynoic acid in the oral cancer tissues compared with the adjacent normal tissues. It need to be confirmed whether these metabolites were derived from oral *Fusobacterium nucleatum* or other microbiota, and their roles in OSCC should be further studied. The effects of metabolites on immune cells within the tumor microenvironment should not be neglected [26–28]. Combined analysis of metabolites data from cancer tissues and saliva indicated decreased D-mannose in the microenvironment of OSCC. It has been recently reported that D-mannose supplementation enhances anti-tumor activity of T cells [28], which implied that decreased D-mannose in OSCC may impair the anti-tumor activity of T cells. However, the specific role of the metabolites in the interaction between microbiota and immune cells within OSCC microenvironment need further investigated.

Conclusions

Collectively, our data showed differential microbiota and metabolites in cancer tissues and saliva from OSCC patients in spite of a small sample size in this study, suggesting an association between some microbiota/metabolite such as *Fusobacterium* or mannose and OSCC. A critical role of microbiota and metabolites in OSCC need to be further investigated.

Abbreviations

HNSCC	Head and neck squamous cell carcinoma
OSCC	Oral squamous cell carcinoma
Fnu	*Fusobacterium nucleatum*
Pgi	*Porphyromonas gingivalis*
Pme	*Prevotella melaninogenica*
CRC	Colorectal cancer
p-EMT	Partial-epithelial mesenchymal transition
OMVs	Outer membrane vesicles
ASV	Amplicon sequence variant
LC-MS/MS	Liquid chromatograph-mass spectrometry/mass spectrometry
GC-MS	Gas chromatograph-mass spectrometry
KEGG	Kyoto Encyclopedia of Genes and Genomes
PCA	Principle component analysis

Supplementary Information

The online version contains supplementary material available at https://doi.org/10.1186/s13027-025-00662-2.

Supplementary Material 1: Table S1. Summary data of raw reads and ASV of 16S rRNA from tissues, saliva and oral swabs.

Supplementary Material 2: Figure S1. KEGG analysis based on the data of 16S rRNA from cancer tissues and PCA of quality control and samples in LC-MS/MS and GC-MS.

Acknowledgements

The authors would thank Liang Pan (Shanghai Ninth People's Hospital) for the help in collecting samples, and the authors would also thank Ziheng Wang and Qidong Zu (Shanghai OE Biotech Co. Ltd.) for their help in data analysis.

Author contributions

Conceptualization: K.W., X.C., F.C., and C.Z.; investigation: K.W., B.X. and X.Z.; formal analysis: B.X., H.G. and G.D.; visualization: K.W., B.X. and X.C.; writing—original draft: K.W. and B.X., writing—review and editing: X.C., F.C., and C.Z.; funding acquisition: X.C. and G.D.; project administration: F.C., C.Z. and X.C.; supervision: X.C. and F.C. All authors have read and agreed to the published version of the manuscript.

Funding
Xu Chen was supported by the Shanghai Pujiang Program (23PJD047), clinical research program (JYLJ202410) and on-job postdoctoral program. Guanhuan Du was supported by the National Natural Science Foundation of China (82101008).

Data availability
The raw sequencing data were posited at the Sequence Read Archive (SRA) with the accession number PRJNA1203737 (For reviewer link-https://dataview.ncbi.nlm.nih.gov/object/PRJNA1203737?reviewer=k6o4m260cfj64atm02bd8d3m1j).

Declarations

Ethics approval and consent to participate
This study was approved by Shanghai Ninth People's Hospital Ethics Committee (SH9H-2024-T252-2).

Consent for publication
All authors and their affiliated institutions have agreed to the publication of this article.

Competing interests
The authors declare no competing interests.

Received: 21 April 2025 / Accepted: 12 May 2025
Published online: 22 May 2025

References

1. Feng X, Luo Q, Zhang H, Wang H, Chen W, Meng G, Chen F. The role of NLRP3 inflammasome in 5-fluorouracil resistance of oral squamous cell carcinoma. J Exp Clin Cancer Res. 2017;36:81.
2. Zhang XY, Shi JB, Jin SF, Wang RJ, Li MY, Zhang ZY, Yang X, Ma HL. Metabolic landscape of head and neck squamous cell carcinoma informs a novel kynurenine/Siglec-15 axis in immune escape. Cancer Commun (Lond). 2024;44:670–94.
3. Amit M, Takahashi H, Dragomir MP, Lindemann A, Gleber-Netto FO, Pickering CR, Anfossi S, Osman AA, Cai Y, Wang R, Knutsen E, Shimizu M, Ivan C, Rao X, Wang J, Silverman DA, Tam S, Zhao M, Caulin C, Zinger A, Tasciotti E, Dougherty PM, El-Naggar A, Calin GA, Myers JN. Loss of p53 drives neuron reprogramming in head and neck cancer. Nature. 2020;578:449–54.
4. Sarkar P, Malik S, Laha S, Das S, Bunk S, Ray JG, Chatterjee R, Saha A. Dysbiosis of oral microbiota during oral squamous cell carcinoma development. Front Oncol. 2021;11:614448.
5. Zhang L, Liu Y, Zheng HJ, Zhang CP. The oral microbiota May have influence on oral Cancer. Front Cell Infect Microbiol. 2019;9:476.
6. Karpinski TM. Role of oral microbiota in Cancer development. Microorganisms. 2019;7:20.
7. Ha NH, Park DG, Woo BH, Kim DJ, Choi JI, Park BS, Kim YD, Lee JH, Park HR. Porphyromonas gingivalis increases the invasiveness of oral cancer cells by upregulating IL-8 and MMPs. Cytokine. 2016;86:64–72.
8. Yu T, Guo F, Yu Y, Sun T, Ma D, Han J, Qian Y, Kryczek I, Sun D, Nagarsheth N, Chen Y, Chen H, Hong J, Zou W, Fang JY. Fusobacterium nucleatum promotes chemoresistance to colorectal Cancer by modulating autophagy. Cell. 2017;170:548–e56316.
9. Rubinstein MR, Wang X, Liu W, Hao Y, Cai G, Han YW. Fusobacterium nucleatum promotes colorectal carcinogenesis by modulating E-cadherin/beta-catenin signaling via its FadA adhesin. Cell Host Microbe. 2013;14:195–206.
10. Jiang SS, Xie YL, Xiao XY, Kang ZR, Lin XL, Zhang L, Li CS, Qian Y, Xu PP, Leng XX, Wang LW, Tu SP, Zhong M, Zhao G, Chen JX, Wang Z, Liu Q, Hong J, Chen HY, Chen YX, Fang JY. Fusobacterium nucleatum-derived succinic acid induces tumor resistance to immunotherapy in colorectal cancer. Cell Host Microbe. 2023;31:781–e7979.
11. Zepeda-Rivera M, Minot SS, Bouzek H, Wu H, Blanco-Miguez A, Manghi P, Jones DS, LaCourse KD, Wu Y, McMahon EF, Park SN, Lim YK, Kempchinsky AG, Willis AD, Cotton SL, Yost SC, Sicinska E, Kook JK, Dewhirst FE, Segata N, Bullman S, Johnston CD. A distinct Fusobacterium nucleatum clade dominates the colorectal cancer niche. Nature. 2024;628:424–32.
12. Li Z, Liu Y, Huang X, Wang Q, Fu R, Wen X, Liu J, Zhang L. F. Nucleatum enhances oral squamous cell carcinoma proliferation via E-cadherin/β-Catenin pathway. BMC Oral Health. 2024;24:518.
13. Geng F, Zhang Y, Lu Z, Zhang S, Pan Y. Fusobacterium nucleatum caused DNA damage and promoted cell proliferation by the Ku70/p53 pathway in oral Cancer cells. DNA Cell Biol. 2020;39:144–51.
14. Shao W, Fujiwara N, Mouri Y, Kisoda S, Yoshida K, Yoshida K, Yumoto H, Ozaki K, Ishimaru N, Kudo Y. Conversion from epithelial to partial-EMT phenotype by Fusobacterium nucleatum infection promotes invasion of oral cancer cells. Sci Rep. 2021;11:14943.
15. Chen G, Gao C, Jiang S, Cai Q, Li R, Sun Q, Xiao C, Xu Y, Wu B, Zhou H. Fusobacterium nucleatum outer membrane vesicles activate autophagy to promote oral cancer metastasis. J Adv Res. 2024;56:167–79.
16. Hooper SJ, Crean SJ, Lewis MA, Spratt DA, Wade WG, Wilson MJ. Viable bacteria present within oral squamous cell carcinoma tissue. J Clin Microbiol. 2006;44:1719–25.
17. Kwak S, Wang C, Usyk M, Wu F, Freedman ND, Huang WY, McCullough ML, Um CY, Shrubsole MJ, Cai Q, Li H, Ahn J, Hayes RB. Oral Microbiome and subsequent risk of head and neck squamous cell Cancer. JAMA Oncol. 2024;10:1537–47.
18. Mäkinen AI, Pappalardo VY, Buijs MJ, Brandt BW, Mäkitie AA, Meurman JH, Zaura E. Salivary Microbiome profiles of oral cancer patients analyzed before and after treatment. Microbiome. 2023;11:171.
19. Pratap Singh R, Kumari N, Gupta S, Jaiswal R, Mehrotra D, Singh S, Mukherjee S, Kumar R. Intratumoral microbiota changes with tumor stage and influences the immune signature of oral squamous cell carcinoma. Microbiol Spectr. 2023;11(4):e0459622.
20. Wei W, Li J, Tang B, Deng Y, Li Y, Chen Q. Metabolomics and metagenomics reveal the impact of Γδ T Inhibition on gut microbiota and metabolism in periodontitis-promoting OSCC. mSystems. 2024;9:e0077723.
21. Liu S, Zhou X, Peng X, Li M, Ren B, Cheng G, Cheng L. Porphyromonas gingivalis promotes immunoevasion of oral Cancer by protecting Cancer from macrophage attack. J Immunol. 2020;205:282–9.
22. Li W, Zhang Z, Wu R, Mao M, Ji Y, Wang X, Dou S, Yan M, Chen W. Fusobacterium nucleatum-Derived outer membrane vesicles promote immunotherapy resistance via changes in Tryptophan metabolism in Tumour-Associated macrophages. J Extracell Vesicles. 2025;14(4):e70070.
23. Yang W, Cong Y. Gut microbiota-derived metabolites in the regulation of host immune responses and immune-related inflammatory diseases. Cell Mol Immunol. 2021;18(4):866–77.
24. Wang H, Rong X, Zhao G, Zhou Y, Xiao Y, Ma D, Jin X, Wu Y, Yan Y, Yang H, Zhou Y, Qian M, Niu C, Hu X, Li DQ, Liu Q, Wen Y, Jiang YZ, Zhao C, Shao ZM. The microbial metabolite trimethylamine N-oxide promotes antitumor immunity in triple-negative breast cancer. Cell Metabol. 2022;34(4):581–e594588.
25. Fan Y, Pedersen O. Gut microbiota in human metabolic health and disease. Nat Rev Microbiol. 2021;19(1):55–71.
26. Cong J, Liu P, Han Z, Ying W, Li C, Yang Y, Wang S, Yang J, Cao F, Shen J, Zeng Y, Bai Y, Zhou C, Ye L, Zhou R, Guo C, Cang C, Kasper DL, Song X, Dai L, Sun L, Pan W, Zhu S. Bile acids modified by the intestinal microbiota promote colorectal cancer growth by suppressing CD8(+) T cell effector functions. Immunity. 2024;57:876–e88911.
27. Jin WB, Xiao L, Jeong M, Han SJ, Zhang W, Yano H, Shi H, Arifuzzaman M, Lyu M, Wang D, Tang YA, Qiao S, Yang X, Yang HS, Fu J, Sonnenberg GF, Collins N, Artis D, Guo CJ. Microbiota-derived bile acids antagonize the host androgen receptor and drive anti-tumor immunity. Cell. 2025;188:2336–e235338.
28. Qiu Y, Su Y, Xie E, Cheng H, Du J, Xu Y, Pan X, Wang Z, Chen DG, Zhu H, Greenberg PD, Li G. Mannose metabolism reshapes T cell differentiation to enhance anti-tumor immunity. Cancer Cell. 2025;43:103–e1218.

Publisher's note